

4

AD-A215 952

AFGL-TR-89-0022
ENVIRONMENTAL RESEARCH PAPERS, NO. 1019

2.7/4.3 Micron CO₂ Branching Ratio Measurement

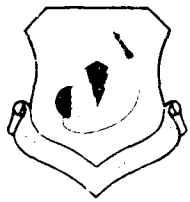
STEVEN M. MILLER



23 January 1989



Approved for public release; distribution unlimited.



DTIC
ELECTE
DEC 13 1989
D



OPTICAL PHYSICS DIVISION PROJECT 2310
AIR FORCE GEOPHYSICS LABORATORY
HANSCOM AFB, MA 01731

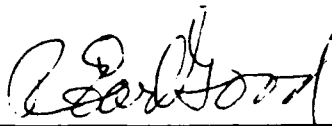
89 12 18 129

"This technical report has been reviewed and is approved for publication"



(Signature)
GEORGE A VANASSE
Branch Chief

FOR THE COMMANDER



(Signature)
R. EARL GOOD
Director

This report has been reviewed by the ESD Public Affairs Office (PA) and is releasable to the National Technical Information Service (NTIS).

Qualified requestors may obtain additional copies from the Defense Technical Information Center. All others should apply to the National Technical Information Service.

If your address has changed, or if you wish to be removed from the mailing list, or if the addressee is no longer employed by your organization, please notify AFGL/DAA, Hanscom AFB, MA 01731. This will assist us in maintaining a current mailing list.

Do not return copies of this report unless contractual obligations or notices on a specific document requires that it be returned.

REPORT DOCUMENTATION PAGE

Form Approved
OMB No. 0704-0188

1. PERSONAL SECURITY CLASSIFICATION Unclassified		1d. RESTRICTIVE MARKINGS	
2. SECURITY CLASSIFICATION AUTHORITY		3. DISTRIBUTION/AVAILABILITY OF REPORT Approved for public release, distribution unlimited.	
3. DECLASSIFICATION/AVOIDANCE SCHEDULE		5. MONITORING ORGANIZATION REPORT NUMBER(S)	
4. MONITORING ORGANIZATION REPORT NUMBER(S) AFGL-TR-89-0022 AFGL, MA, 01119		7a. NAME OF MONITORING ORGANIZATION	
5. NAME OF PERFORMING ORGANIZATION Air Force Geophysics Laboratory	6a. OFFICE SYMBOL (If applicable) OPI	7b. ADDRESS (City, State, and ZIP Code)	
6b. ADDRESS (City, State, and ZIP Code) Hanscom AFB Massachusetts 01731-5000		9. PROCUREMENT INSTRUMENT IDENTIFICATION NUMBER	
7. NAME OF FUNDING / SPONSORING ORGANIZATION Air Force Geophysics Laboratory	8a. OFFICE SYMBOL (If applicable) OPI	10. SOURCE OF FUNDING NUMBERS	
8b. ADDRESS (City, State, and ZIP Code) Hanscom AFB Massachusetts 01731-5000		PROGRAM ELEMENT NO. 61102F	PROJECT NO. 2310
		TASK NO. G4	WORK UNIT ACCESSION NO. 19
11. TITLE (Include Security Classification) (U) 2.7/4.3 Micron CO ₂ Branching Ratio Measurement			
12. PERSONAL AUTHOR(S) Miller, S.M.			
13a. TYPE OF REPORT Scientific Interim	13b. TIME COVERED FROM 6/84 TO 6/87	14. DATE OF REPORT (Year, Month, Day) 1989 January 23	15. PAGE COUNT 30
16. SUPPLEMENTARY NOTATION <i>cont'd from pg. 1</i>			
17. COSATI CODES		18. SUBJECT TERMS (Continue on reverse if necessary and identify by block number)	
FIELD 04	GROUP 01	Branching Ratio Interferometry, Resonant fluorescence, CO ₂ Emission Laser Excitation Emission Spectra	
19. ABSTRACT (Continue on reverse if necessary and identify by block number) The radiative branching ratio from the CO ₂ (021) combination vibrational energy state to the CO ₂ (020) and CO ₂ (000) states is measured using both laser induced fluorescence excitation and spectrally resolved fluorescence experiments. These measurements bound the branching ratio (CO ₂ (021) → CO ₂ (020) / CO ₂ (021) → CO ₂ (000)) between 13 and 16. Keywords:			
BEST AVAILABLE COPY			
20. DISTRIBUTION/AVAILABILITY OF ABSTRACT <input type="checkbox"/> UNCLASSIFIED/UNLIMITED <input checked="" type="checkbox"/> SAME AS RPT <input type="checkbox"/> DFC USERS		21. ABSTRACT SECURITY CLASSIFICATION Unclassified	
22a. NAME OF RESPONSIBLE INDIVIDUAL S.M. Miller		22b. TELEPHONE (Include Area Code) 617-377-2810	22c. OFFICE SYMBOL AFGL/OPI

Accession For	
NTIS GRA&I	<input checked="" type="checkbox"/>
DTIC TAB	<input type="checkbox"/>
Unannounced	<input type="checkbox"/>
Justification	
By	
Distribution/	
Availability Codes	
Dist	Avail and/or Special
A-1	



Contents

1. INTRODUCTION	i
2. EXPERIMENTAL	2
3. RESULTS	4
3.1 Photoacoustic	4
3.2 Fluorescence Excitation	4
3.3 Absorption	11
3.4 Fluorescence Spectra	11
4. SPECTRAL MODELING	15
5. DISCUSSION	15
6. CONCLUSION	23
REFERENCES	25

Illustrations

1. Partial Energy Level Diagram for CO ₂	3
2. Photoacoustic/Fluorescence Excitation Experimental Setup	5
3a. Fluorescence Excitation Experimental Setup	6
3b. Interferometric Experimental Setup	7
4. Photoacoustic Spectrum	8
5. Fluorescence Excitation Spectrum - 1 Torr CO ₂	9
6. Fluorescence Excitation Spectrum - 20 Millitorr CO ₂	10
7. Fluorescence Excitation Spectrum - 2.7 μm Bandpass - CO ₂	12
8. Fluorescence Excitation Spectrum - 2.7 μm Bandpass - No CO ₂	13
9. Fluorescence Spectrum - 2000 - 4000 cm ⁻¹ CO ₂ 50 Millitorr	14
10. Fluorescence Spectrum 2200 - 2400 cm ⁻¹ CO ₂ 20 Millitorr to 1.1 Torr 4.3 μm Band	16
11. 50 mt	17
12. 0.1 t	18
13. 0.5 t	19
14. 1.1 t	20
15. Spectral Fits	21

Table

1. Calculated Integrated Intensity of Vibrational Bands	22
---	----

2.7/4.3 Micron CO₂ Branching Ratio Measurement

1. INTRODUCTION

Two rocket infrared measurement programs during the 1970's (ICE CAP and SPIRE) measured significant amounts of radiation in the upper atmosphere at 2.7 microns.^{1,2,3,4} Several papers have been published^{5,6} which attribute this radiation at 2.7 μm to the hot bands of CO₂. To determine the contribution of 2.7 μm radiation from CO₂, each of these analyses rely on a simple theoretical calculation of the CO₂ branching ratio between 2.7 μm and 4.3 μm .

$$\frac{A(4.3 \mu\text{m})}{A(2.7 \mu\text{m}) + A(4.3 \mu\text{m})} = \frac{(v_{4.3})^2 * S_{4.3}}{(v_{2.7})^2 * S_{4.3} + (v_{2.7})^2 * S_{4.3}} = 0.96$$

(Received for publication 20 January 1989)

1. Stair, A.T., Jr., Ulwick, J.C., Baker, K.D., and Baker, D.J. (1975) Rocketborne observations of atmospheric infrared emissions in the auroral region, *Atmospheres of Earth and Planets*, ed. McCormac, B.M., Reidei, D., Dordrecht, Netherlands.
2. Kumer, J.B. (1974) *Analysis of 4.3 Micron ICE CAP Data*, Air Force Cambridge Res. Lab., Bedford, MA, AFCRL-TR-74-0334, ADA014847.
3. Sharma, R.D., Nadile, R., Stair, A.T., Jr., and Gallery, W. (1981) Earth limb emission analysis of Spectral Infrared Rocket Experiment (SPIRE) data at 2.7 micrometers, *Modern Utilization of Infrared Technology, Proc. Soc. Photo Opt. Instrum. Eng.* **304**:139-142.
4. Stair, A.T., Jr., Sharma, R.D., Nadile, R.M., Baker, D.J., and Grieder, W.F. (1985) Observation of limb radiance with cryogenic Spectral Infrared Rocket Experiment (SPIRE), *J. Geophys. Res.* **90**:(A10).
5. Kumer, J.B. (1977) Theory of the CO₂ 4.3 Aurora Related Phenomena, *J. Geophys. Res.* **82**:(16).
6. Sharma, R.D. (1985) CO₂ Component of Daytime Earth Limb Emission at 2.7 Micrometers, *J. Geophys. Res.* **90**:(A10).

where A is the Einstein A coefficient, ν is the frequency in wavenumber and S is the transition line strength.

Examination of Figure 1 shows that there are two assumptions built into this calculation. The line strengths of the $101 \rightarrow 100$ and $021 \rightarrow 020$ have not been measured. Thus it is assumed since only one quanta of asymmetric stretch is changing, that the following matrix elements are equal: $\langle 101|u|100 \rangle = \langle 021|u|020 \rangle = \langle 001|u|000 \rangle$, where u is the dipole moment operator. It is also assumed that the line strengths for radiation at $4.26 \mu\text{m}$, $2.7 \mu\text{m}$, and $2.77 \mu\text{m}$ are known accurately. Both these assumptions can be avoided by measuring the branching ratio experimentally.

James and Kumer^{7,8} attempted to confirm this branching ratio experimentally, first by observing $4.3 \mu\text{m}$ radiation from a low pressure CO_2 cell when radiated by blackbody radiation and later by observing fluorescence decays when a pulsed laser source at $2.7 \mu\text{m}$ is used.

An inherent problem with this experiment is its inability to discriminate $4.3 \mu\text{m}$ radiation from the $101 \rightarrow 100$, and $021 \rightarrow 020$ transitions from the $001 \rightarrow 000$ transition. The 001 energy level becomes populated by collisional excitation which is not important in the upper atmosphere above 50 km but is very important under the 300 mTorr pressures utilized in these experiments. This lack of discrimination prevents the proper determination of the $4.3/2.7 \mu\text{m}$ branching ratio.

The experiment described here solves this problem by spectrally resolving the direct radiation from the 101 and 021 energy levels from the radiation due to the collisional coupling with the 001 band.

2. EXPERIMENTAL

This project consisted of four experiments. These were an IR absorption measurement to confirm the absorption coefficient (and thus the absorption cross section), a photoacoustic measurement to identify the rotational lines of the absorbed $2.7 \mu\text{m}$ radiation, a fluorescence excitation experiment to determine the sensitivity of this method, and an interferometry experiment to spectrally resolve the fluorescence from the CO_2 . All of these experiments utilized a Burleigh model FCL-20 Kr+ laser pumped F-center laser to obtain approximately 50 milliwatts of infrared radiation continuously tunable from $2.5 \mu\text{m}$ to $2.75 \mu\text{m}$. This laser was operated multimode to scan through the $2.7 \mu\text{m}$ absorption region of CO_2 and was operated in single mode to obtain an absorption measurement on a single rotational line. All data were acquired, displayed, stored and analyzed on a Hewlett-Packard model 9836 computer equipped with a multiprogrammer to scan the laser and acquire data.

The photoacoustic measurements were made using a hearing aid microphone positioned via a "spider" near the center axis of an MDC model 150-4 gas cell equipped with 1 inch sapphire windows. The laser beam was chopped using a PTI model 4000 tuning fork chopper at 400 Hz and passed through

7. James, T.C. (1976) *Laboratory Investigation of Infrared Fluorescence of CO_2* , HAES Report No. 60, Final Report to DNA 4238F, Cont. DNA 001-76-C-0017, ADA043524.

8. James, T.C. and Kumer, J.B. (1979) *Fluorescence Experimental and Auroral Data Evaluation to Improve Prediction of Nuclear Atmospheric Infrared Background*, DNA Report LMSC/D673384, ADA085724.

CO₂ 4.3 Micron Earth Limb Fluorescence

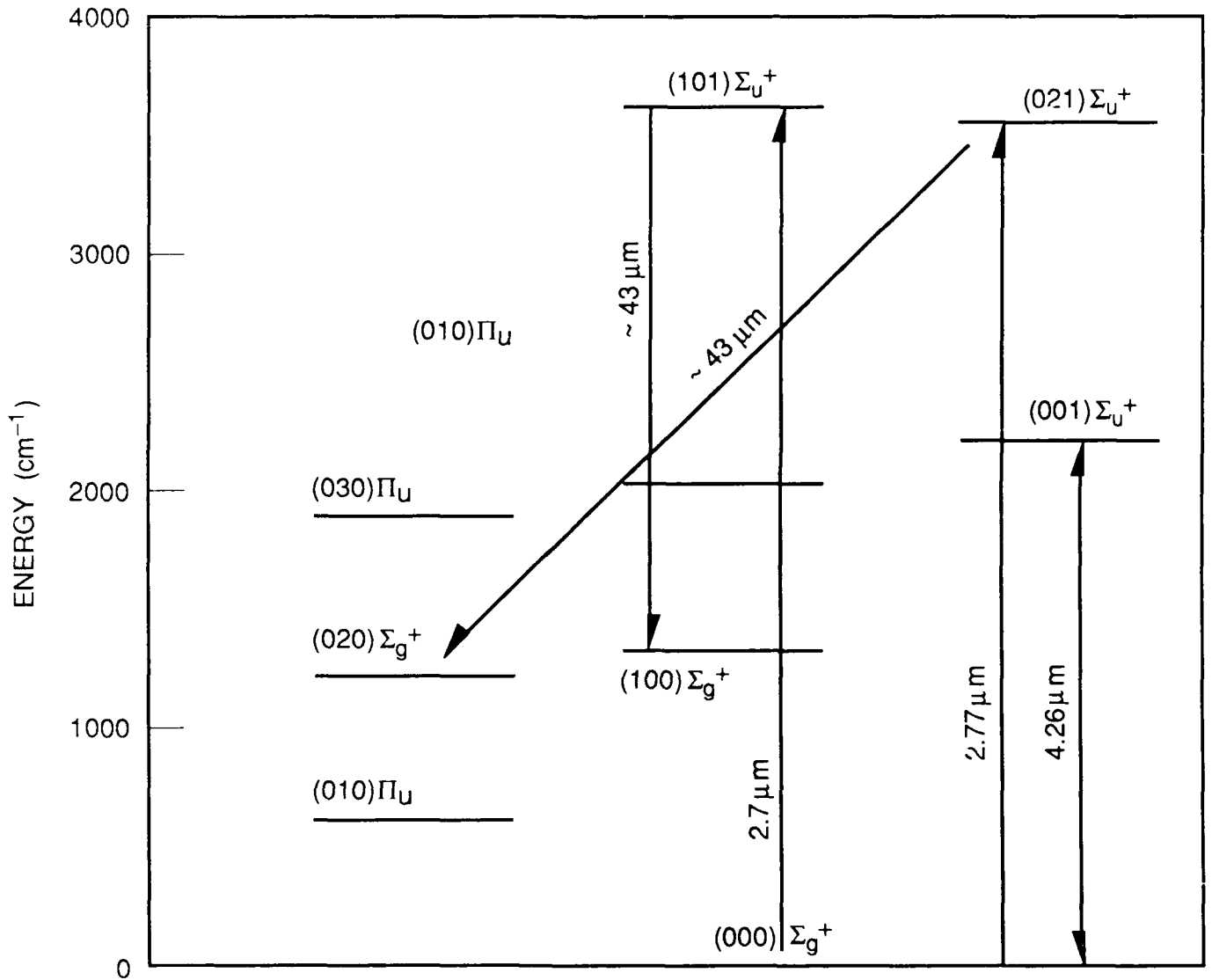


Figure 1. Partial Energy Level Diagram for CO₂

the gas cell along a horizontal axis and terminated on a Scientech model 365 power meter. The microphone signal was pre-amplified using a model 747 operational amplifier and fed into a Stanford Research model SP 510 lockin amplifier. The signal from the lockin was sent to the HP computer. Matheson grade CO₂ and UHP grade argon were used throughout without further purification. The photoacoustic signal was obtained at 100 torr of CO₂ with no buffer gas.

The absorption experiment utilized the F-center laser, the photoacoustic gas cell, and the Scientech Power meter. The laser was tuned to the peak of a strong rotational line. Laser power was measured after the beam passed through the gas cell with and without CO₂ in the cell. This provides the relative powers necessary to calculate the absorption cross section.

The equipment arrangement for the photoacoustic and absorption experiment is shown in Figure 2. The fluorescence excitation experiment utilized a fluorescence cell with Brewster angle windows and baffling to reduce laser beam scattering to a minimum, and a recessed observation window capable of holding various bandpass filters and/or lenses to couple to the InSb infrared detector. The laser beam path between the laser and the cell was purged with N₂. The fluorescence from the cell was collected as the F-center laser was tuned through the (021) combination band of CO₂, 2.640 μm to 2.730 μm. The equipment arrangement for this experiment is shown in Figure 3a.

The spectrally resolved fluorescence was observed using a Michelson interferometer with a spectral resolution of 8 cm⁻¹ using the arrangement shown in Figure 3b. Both the laser path and the path from the cell to the interferometer were purged with N₂ to eliminate both water vapor and atmospheric CO₂. The interferometer was calibrated using both a blackbody source and a helium lamp for both relative and absolute spectral response. The cell was evacuated and heated and a baseline was taken at least on a daily basis with less than 0.1 μm background pressure. Spectra were collected at several pressures between 10 millitorr and 10 torr with and without Ar buffer gas.

3. RESULTS

3.1 Photoacoustic

A typical photoacoustic spectrum is shown in Figure 4. This represents the nonradiative portion of the energy absorbed by the CO₂ into the (021) combination band. The rotational assignments can be made by identifying the gap between the R and P branches of the spectrum. This spectrum required 100 torr of CO₂ in the cell and 20 - 30 mw of FCL radiation scanned from 2.64 to 2.73 μm. The deviation from regularity on the R branch side results from laser beam absorption by water vapor. Although the laser path is purged with N₂, water has a very large absorption coefficient for 2.7 μm radiation. Using this spectrum, the P11 rotational line was chosen for the fluorescence experiments.

3.2 Fluorescence Excitation

The next stage involved observing the total fluorescence in the 4.3 μm bandpass from the absorption of 2.7 μm radiation. Figures 5 and 6 show this 4.3 μm fluorescence as a function of laser wavelength. The first spectrum required 80 mw of laser radiation, 1 torr of CO₂ and 50 torr of Argon buffer gas, while the second required 90 mw of laser radiation, 20 torr of CO₂ and 50 torr of Argon

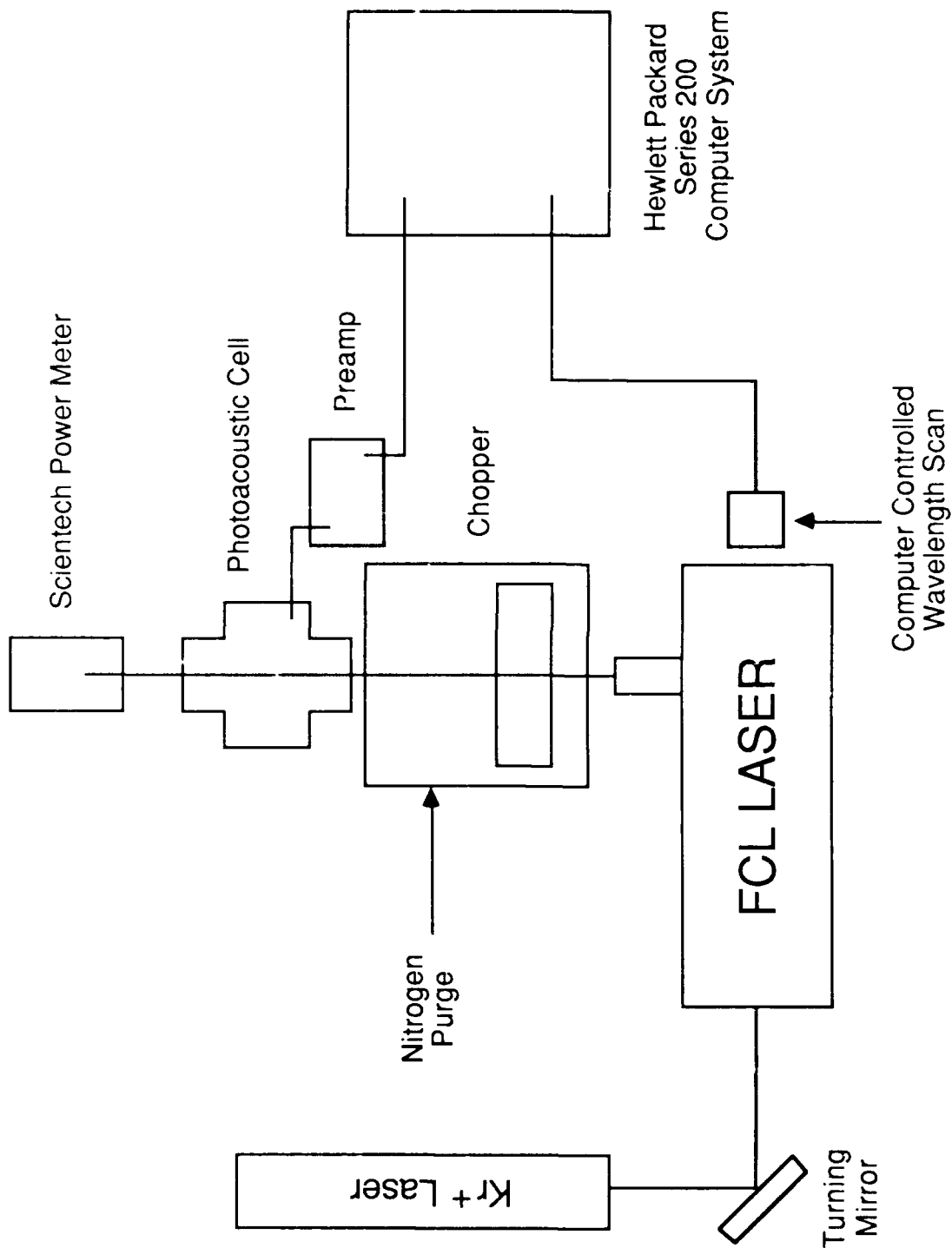


Figure 2. Photoacoustic/Fluorescence Excitation Experimental Setup

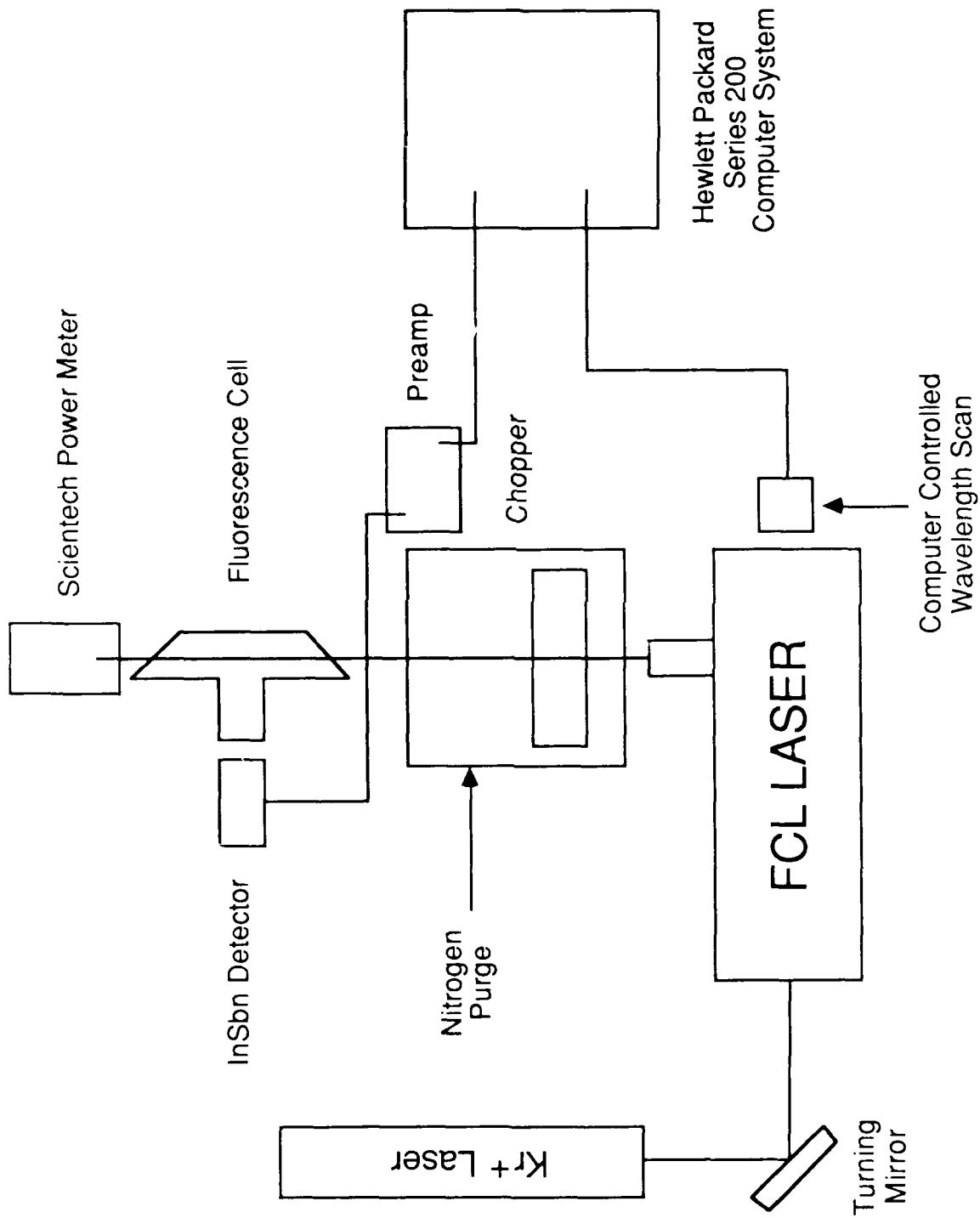


Figure 3a. Fluorescence Excitation Experimental Setup

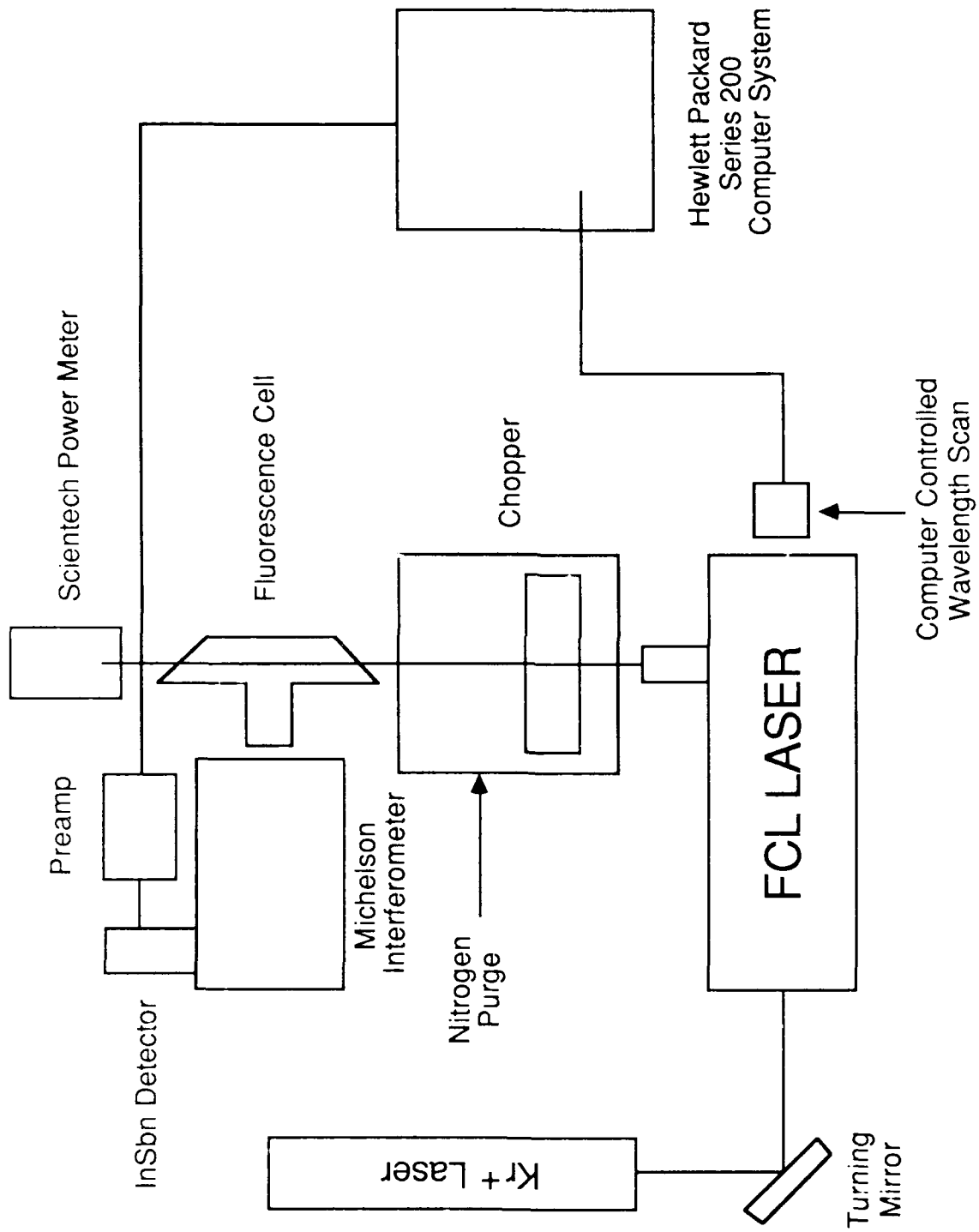


Figure 3b. Interferometric Experimental Setup

CO₂ Photoacoustic

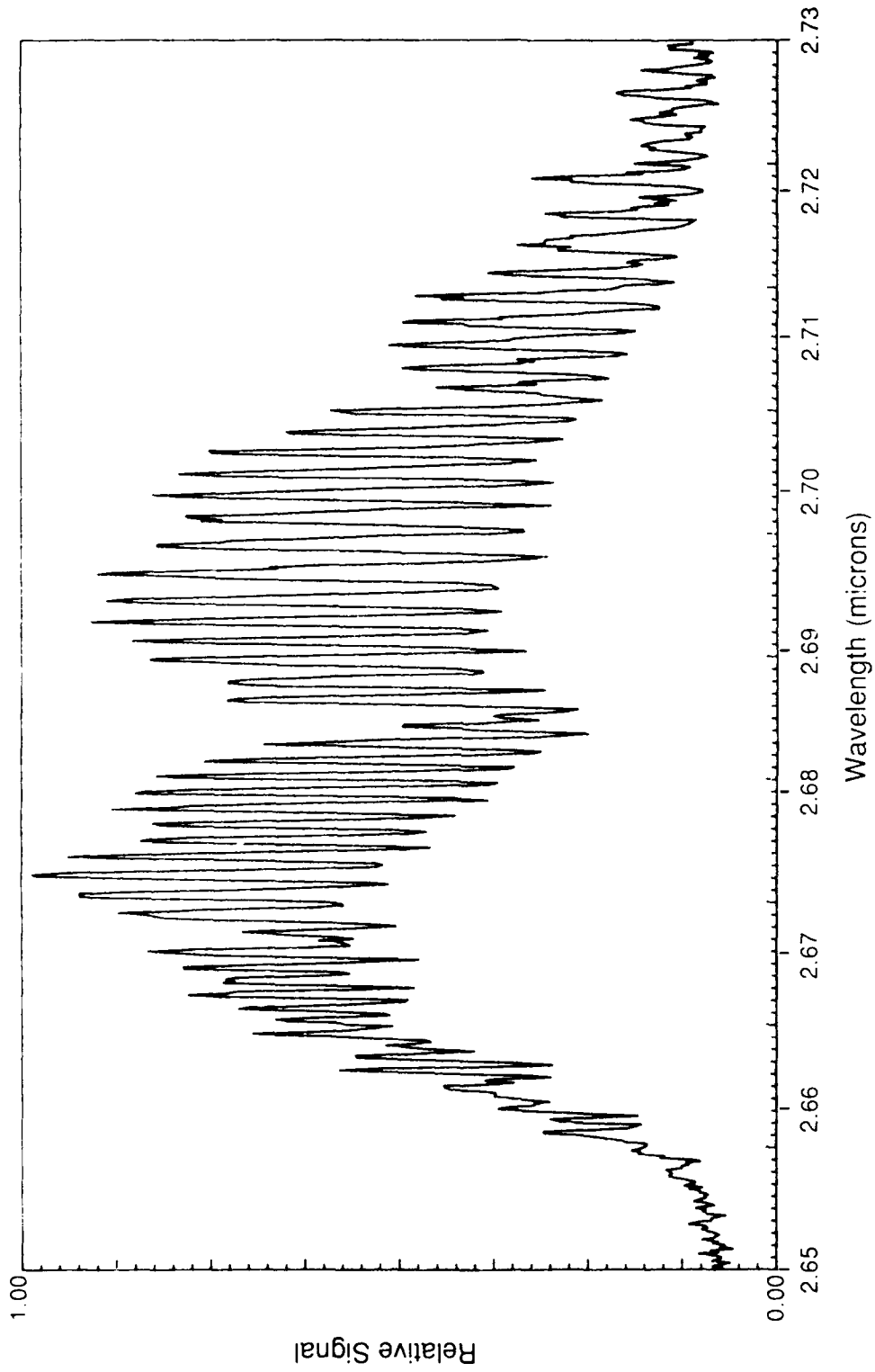


Figure 4. Photoacoustic Spectrum

CO₂ Fluorescence Excitation
1 Torr CO₂, 50 Torr AR

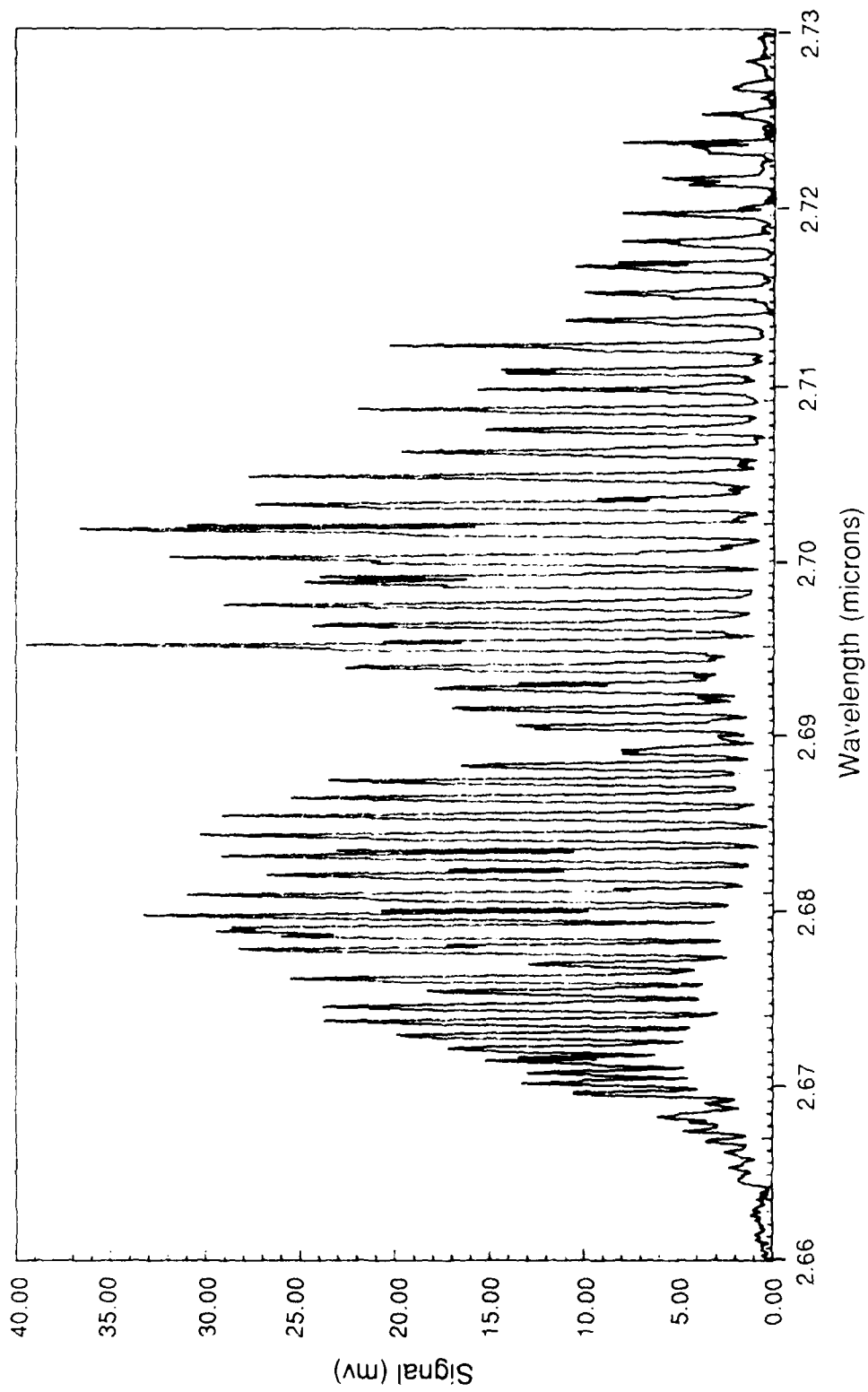


Figure 5. Fluorescence Excitation Spectrum - 1 Torr CO₂

CO₂ Fluorescence Excitation
20 millitorr CO₂, 50 Torr AR

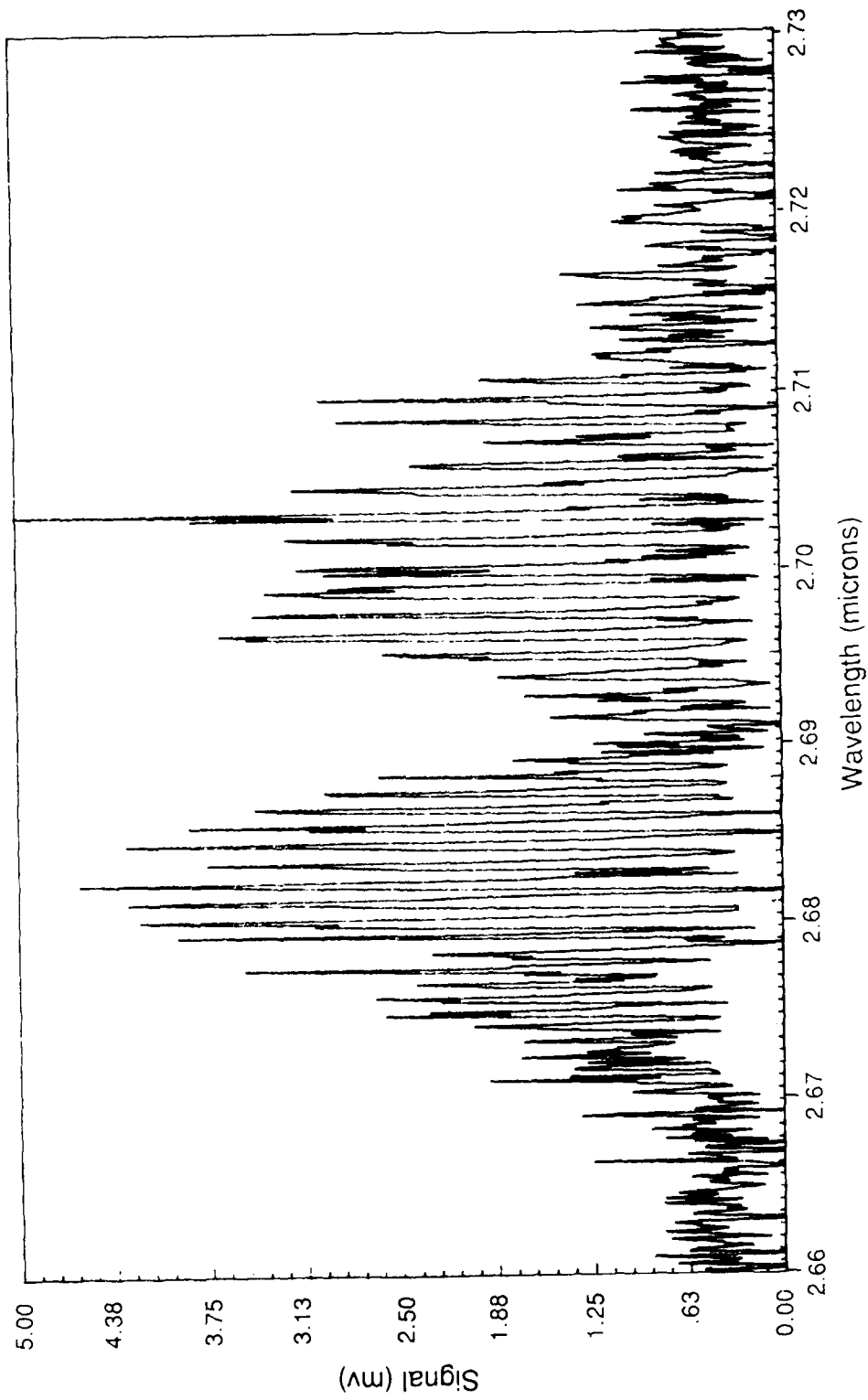


Figure 6. Fluorescence Excitation Spectrum - 20 Millitorr CO₂

buffer gas. These spectra clearly show that a pressure range of 10 millitorr to 10 torr of CO₂ could be studied with sufficient signal to noise to determine the CO₂ branching ratio. Fluorescence in the 2.7 μm bandpass was examined with less success. To discriminate 2.7 μm fluorescence from laser radiation, a short wavelength R branch rotational line had to be excited and the longer wavelength P branch fluorescence observed. This ideally requires a bandpass filter with a very sharp short wavelength cutoff. Without such an ideal filter the 2.7 μm fluorescence has to be extracted from a large laser background at 2.7 μm. This is evident in Figure 7 where a 2.7 μm bandpass is used and a fluorescence excitation spectrum has been obtained. The 2.7 μm fluorescence is manifested as the small rotational structure on a large 2.7 μm laser scattered background (with water absorption lines). This spectrum can be compared to the one in Figure 8 where only Argon buffer gas is in the cell and all other conditions remain the same. Here the oscillations are not observed. This data demonstrates that it is difficult to observe the 2.7 μm fluorescence even without the losses associated with further spectral discrimination.

The intensity of the 4.3 μm data on the same experimental run is 112 mv vs 2 mv intensity of the 2.7 μm structure under the same conditions, 1 torr CO₂ and 50 torr Ar. The bandpass filters at 4.3 μm and 2.7 μm have the same throughput while the InSb detector is a factor of 1.5 times more sensitive at 4.3 μm than 2.7 μm.

3.3 Absorption

The absorption study was hampered by the dual mode radiation of the FCL. Since the FCL uses a near hemispheric resonator, a standing wave is set up in the cavity. This standing wave causes a second "hole-burning" mode to compete with the original mode. The spacing between these two modes is 10 GHz. When the absorption is measured using this dual mode of FCL operation, the mode tuned to the peak of a rotation line is absorbed significantly more than the mode not in resonance with a rotational line. The results become too convolved to perform the measurement properly. Therefore, an etalon was inserted into the FCL cavity to eliminate the "hole-burning" mode. This involved carefully controlling the length of the cavity, the distance between etalon surfaces and the grating position. A second etalon was used outside the cavity to measure the mode spacing and detect the presence of one or two modes. The nonorthogonal nature of this elaborate tuning scheme resulted in the ability to either obtain single mode tuning at a nonspecific wavelength or to obtain a specific wavelength with both modes. It was very difficult to obtain single frequency operation at a desired wavelength. Thus, this portion of the experiment was abandoned in favor of accepting the absorption cross sections published in DNA report #4238F by T.C. James.

3.4 Fluorescence Spectra

The final experimental step to determine the 4.3/2.7 μm branching ratio is resolving the CO₂ fluorescence into the following transitions; (021 → 020) at 4.3 μm, (021 → 000) at 2.7 μm, and (001 → 000) at 4.26 μm. This is accomplished using a calibrated Michelson interferometer as described in the experimental section. The results at 2.7 μm are shown in Figure 9. All features in this spectral region at all pressures investigated (20 mtorr to 10 torr) can be attributed to scattered laser light. This lack of

CO₂ Fluorescence Excitation
1 Torr CO₂, 50 Torr AR, 2.7 μm Filter

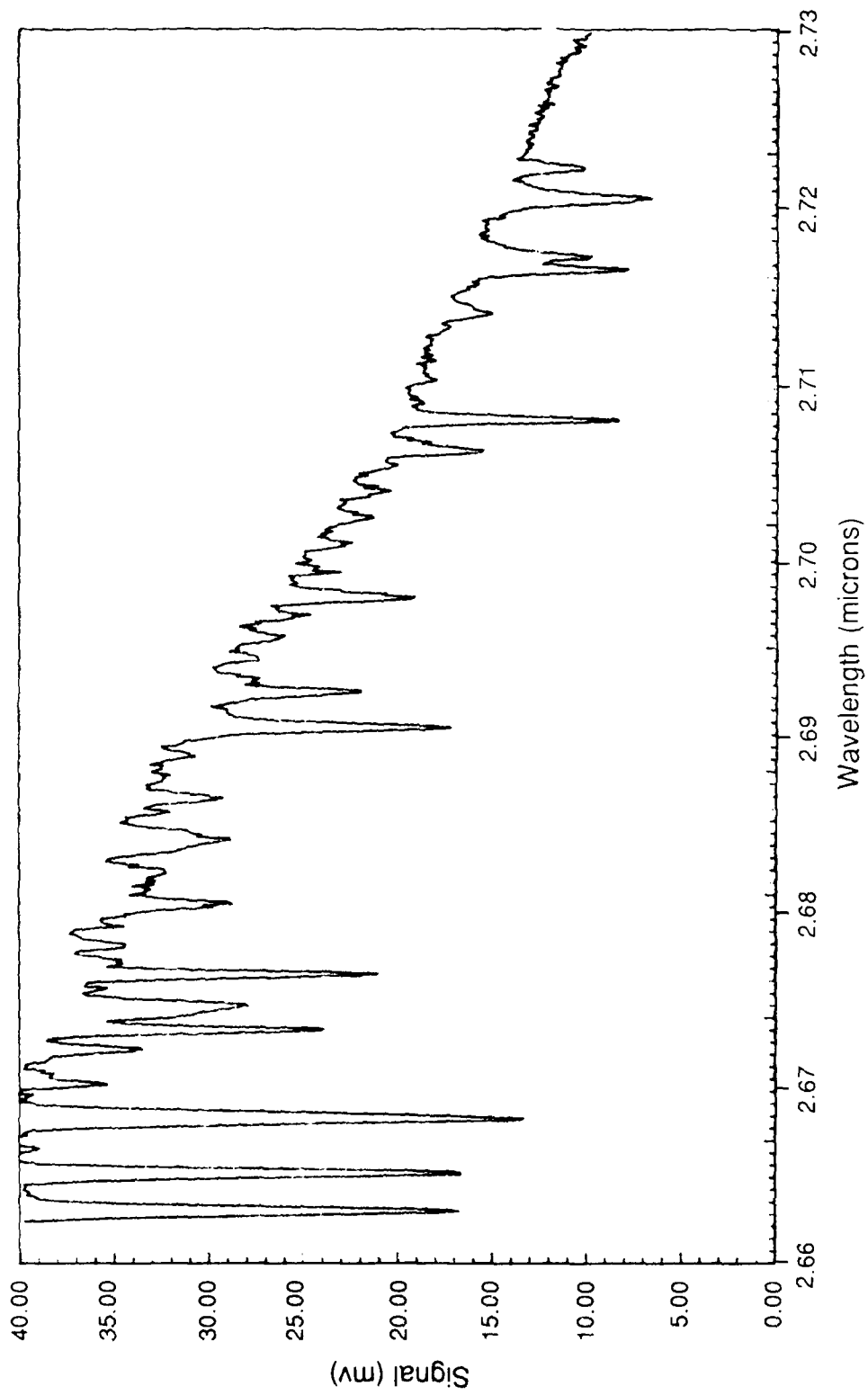


Figure 7. Fluorescence Excitation Spectrum - 2.7 μm Bandpass - CO₂

Background 2.7 Micron Filter

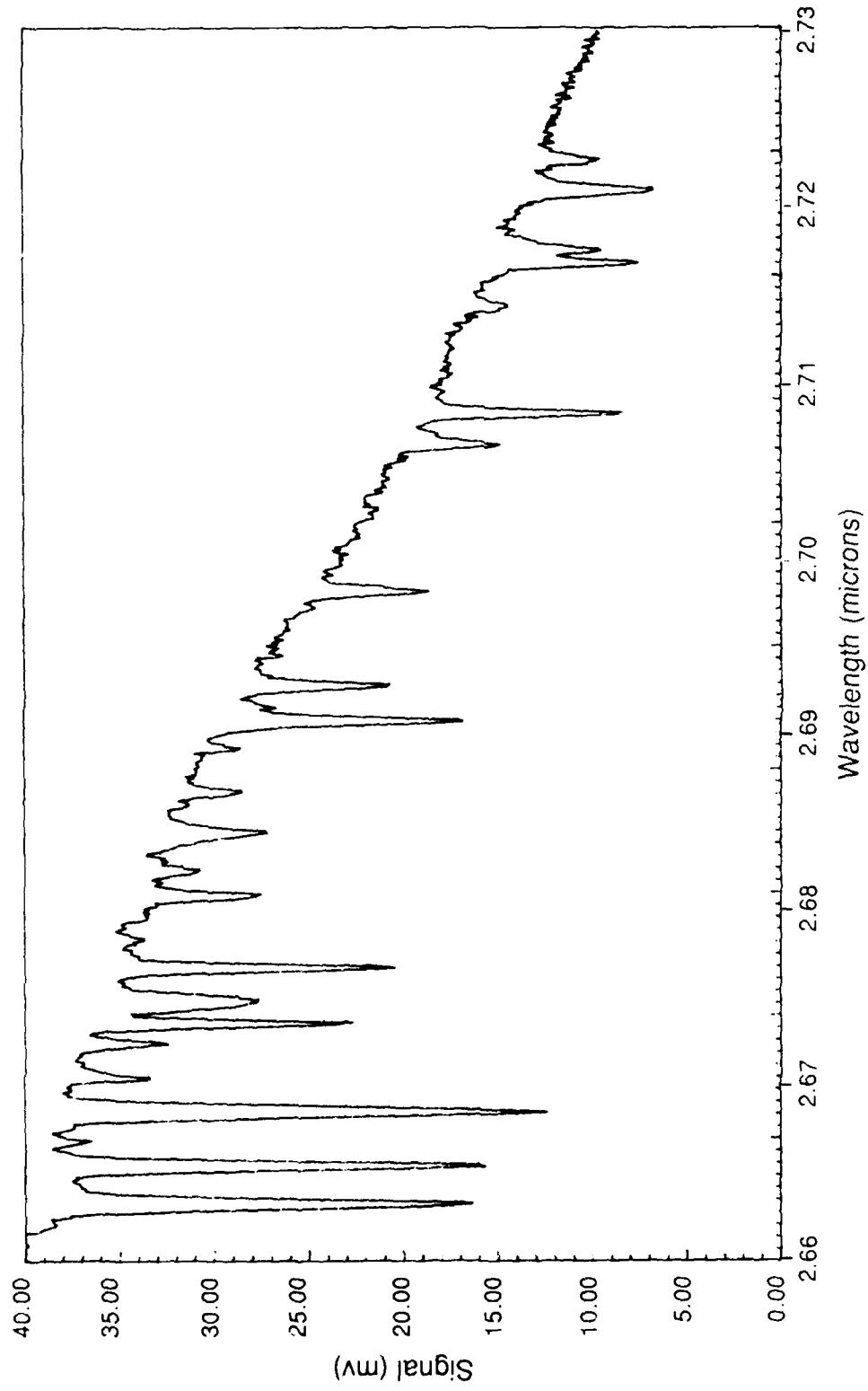


Figure 8. Fluorescence Excitation Spectrum - 2.7 μm Bandpass - No CO_2

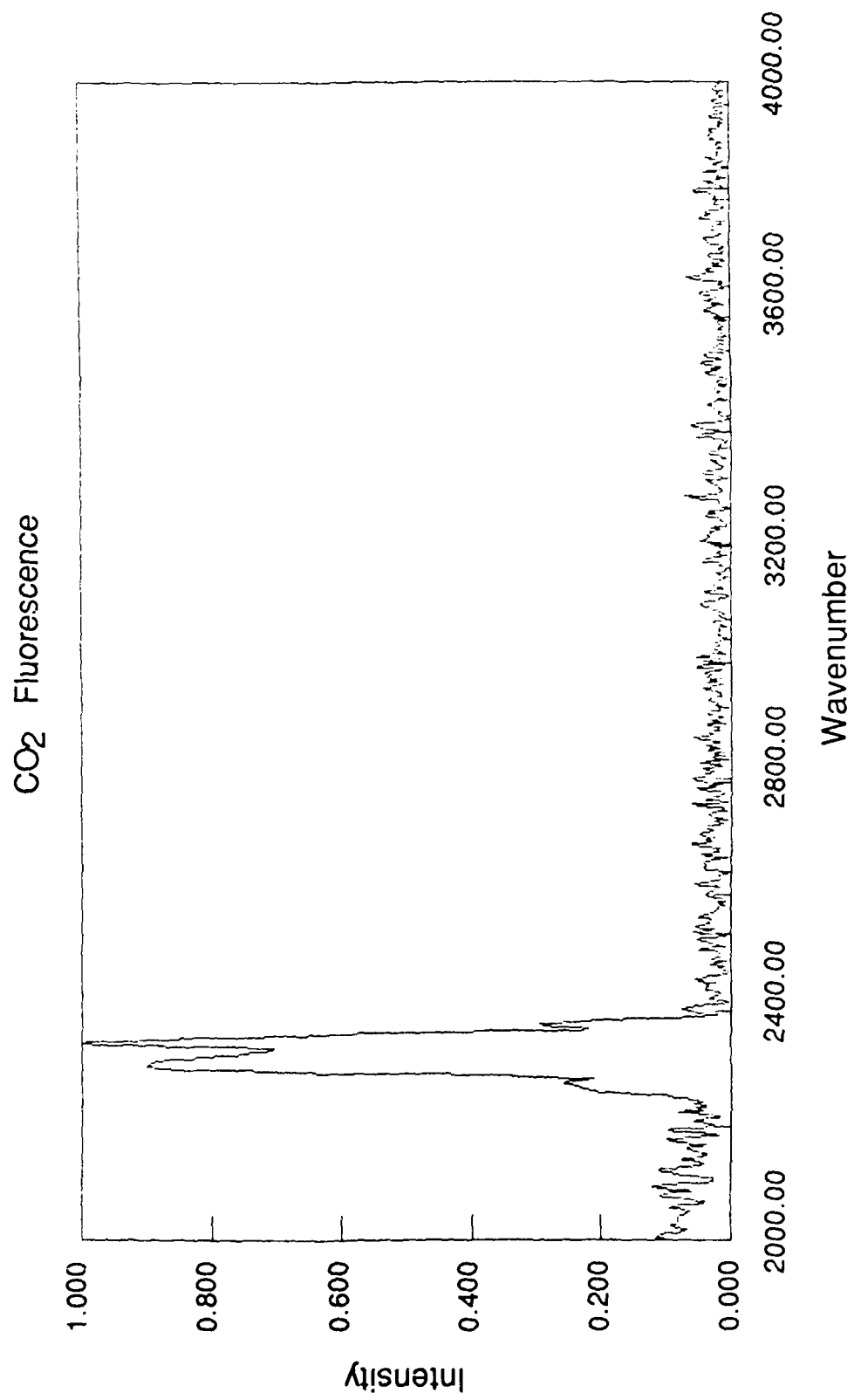


Figure 9. Fluorescence Spectrum - 2000 - 4000 cm⁻¹ CO₂ 50 Millitorr

any fluorescence at 2.7 μm [or at 2.77 μm - the Fermi resonant (101 \rightarrow 000) transition] limits the results to predicting a lower limit of the 4.3/2.7 μm CO_2 branching ratio. The fluorescence results near 4.3 μm are shown in Figures 10 to 14. The 8 cm^{-1} instrument resolution provides the R and P branch envelopes without resolving the individual rotational lines. As can be seen most clearly in Figure 14, there are at least 2 overlapping vibrational bands observed. In order to determine which CO_2 bands contributed to these spectra a synthetic spectral modeling program was written, with a linear least squares fitting routine after Bevington⁹ utilized. All data on vibrational transition probabilities, rotational line widths and positions were taken from the HITRAN¹⁰ database at AFGL.

4. SPECTRAL MODELING

The basic flow of the program used for this modeling is as follows. Both experimental data and the rotational line positions, line strengths, and line widths of the CO_2 bands of interest from the HITRAN database are input to the program. The HITRAN line strength data is converted to Einstein A coefficients, the spectral line shape is determined using the linewidths, the sinc function response of the interferometer, and the appropriate line shape function for the pressure. These are a Doppler lineshape for pressures < 10 mtorr, a Lorentz lineshape for pressures > 10 torr and Voigt profile for pressures less than 10 torr and greater than 10 mtorr. The individual rotational lines are then combined with an appropriate resolution to form the respective vibrational band. If the vibrational band to be calculated is connected to the ground state, then an optical thickness parameter is calculated using equations derived in References 11 and 12. Each broadening mechanism (Doppler, Lorentzian, or Voigt) requires a unique calculation of the optical thickness. This optical thickness parameter ($0 < \gamma < 1$) becomes a multiplicative factor for the intensity of each wavelength point in the vibrational band. The fundamental band together with several hot and isotope bands form a basis set that can be fit to the experimental data. A linear least squares fitting routine calculates the relative amounts of each vibrational band in the basis set necessary to best fit the experimental data. An example of these fits is shown in Figure 15.

5. DISCUSSION

The main difficulty in what might be considered a rather straightforward molecular energy level branching ratio experiment remains a significant overlapping spectral contribution from radiating energy levels, populated solely by collisions (particularly the 001 \rightarrow 000 transition). Although this

-
9. Bevington, P.R. (1969) *Data Reduction and Error Analysis for the Physical Sciences*, McGraw-Hill.
 10. Rothman, L.S., and Young, L.D.G. (1981) Infrared Energy Levels and Intensities of Carbon Dioxide - II, *J. Quant. Spectrosc. Radiat. Trans.* **25**:505-524.
 11. Caledonia, G.E., Green, B.D., and Murphy, R.E. (1982) On self-trapping of $\text{CO}_2(\nu_3)$ fluorescence, *J. Chem. Phys.* **77**:(10).
 12. Green, B.D., Caledonia, G.E., Piper, L.G., Goela, J.S., Fairbairn, A., and Murphy, R.E. (1981) *LABCEDE Studies*, AFGL-TR-82-0060, ADA114389.

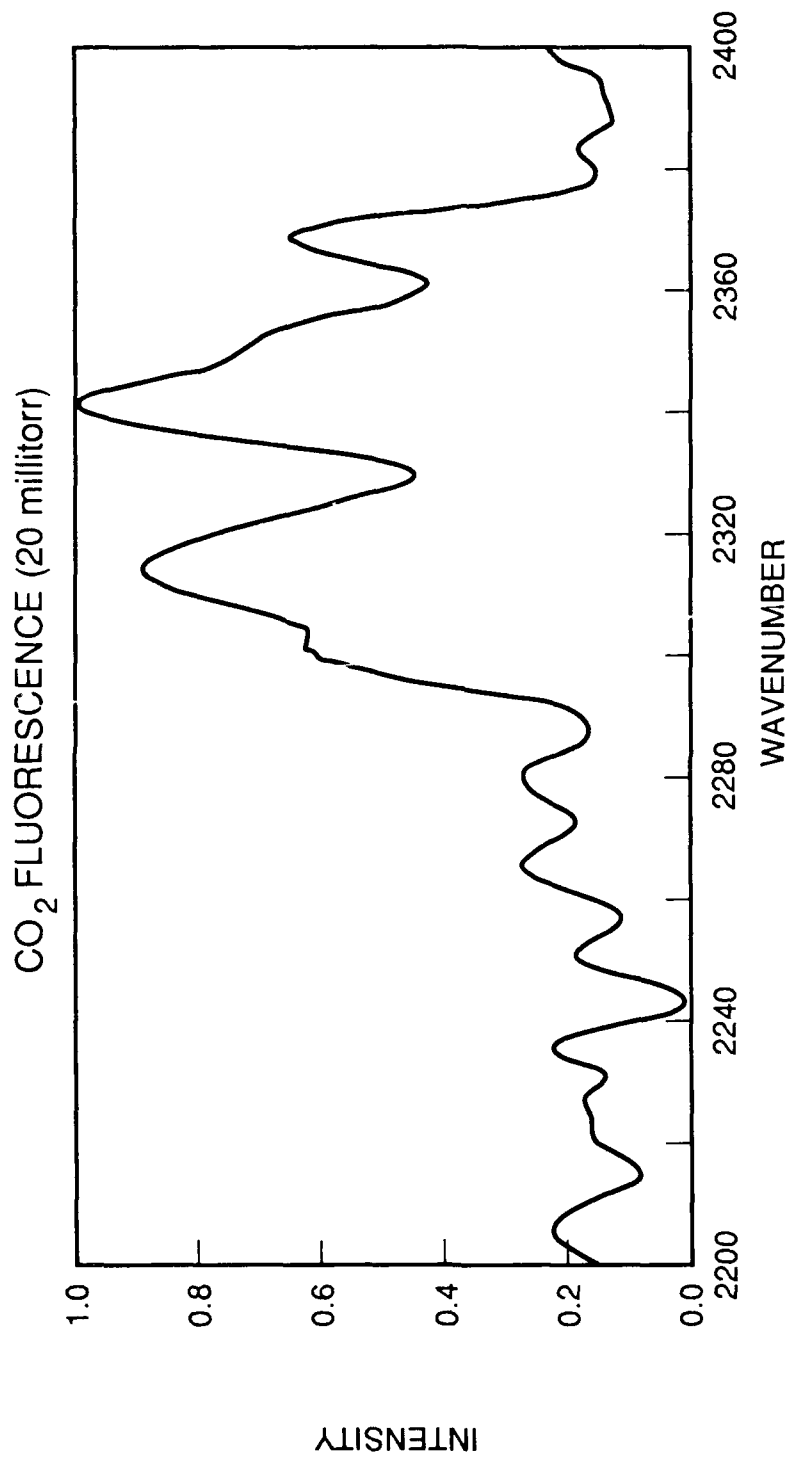


Figure 10. Fluorescence Spectrum - 2200 - 2400 cm⁻¹ CO₂ 20 Millitorr to 1.1 Torr 4.3 μm Band

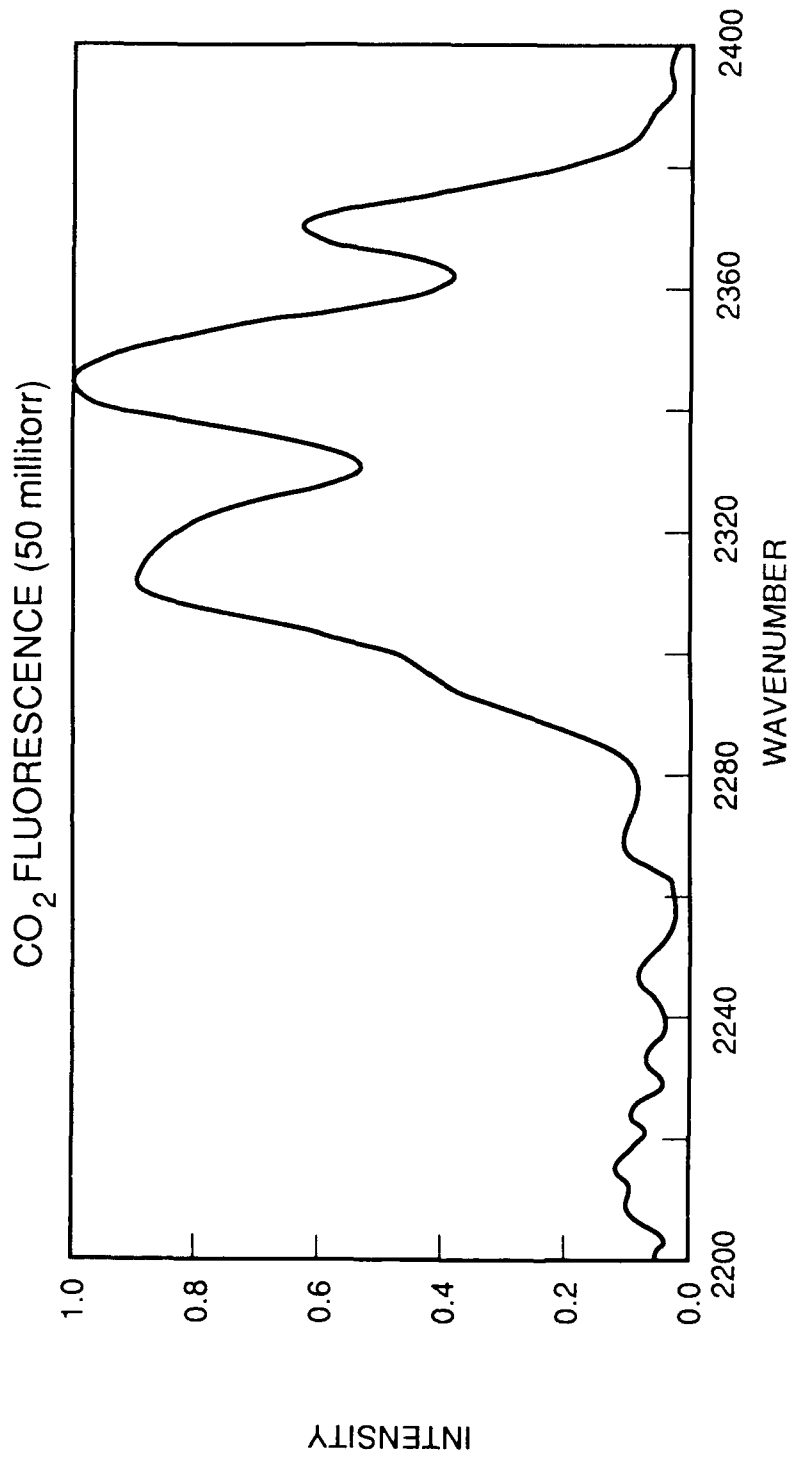


Figure 11. 50 mt

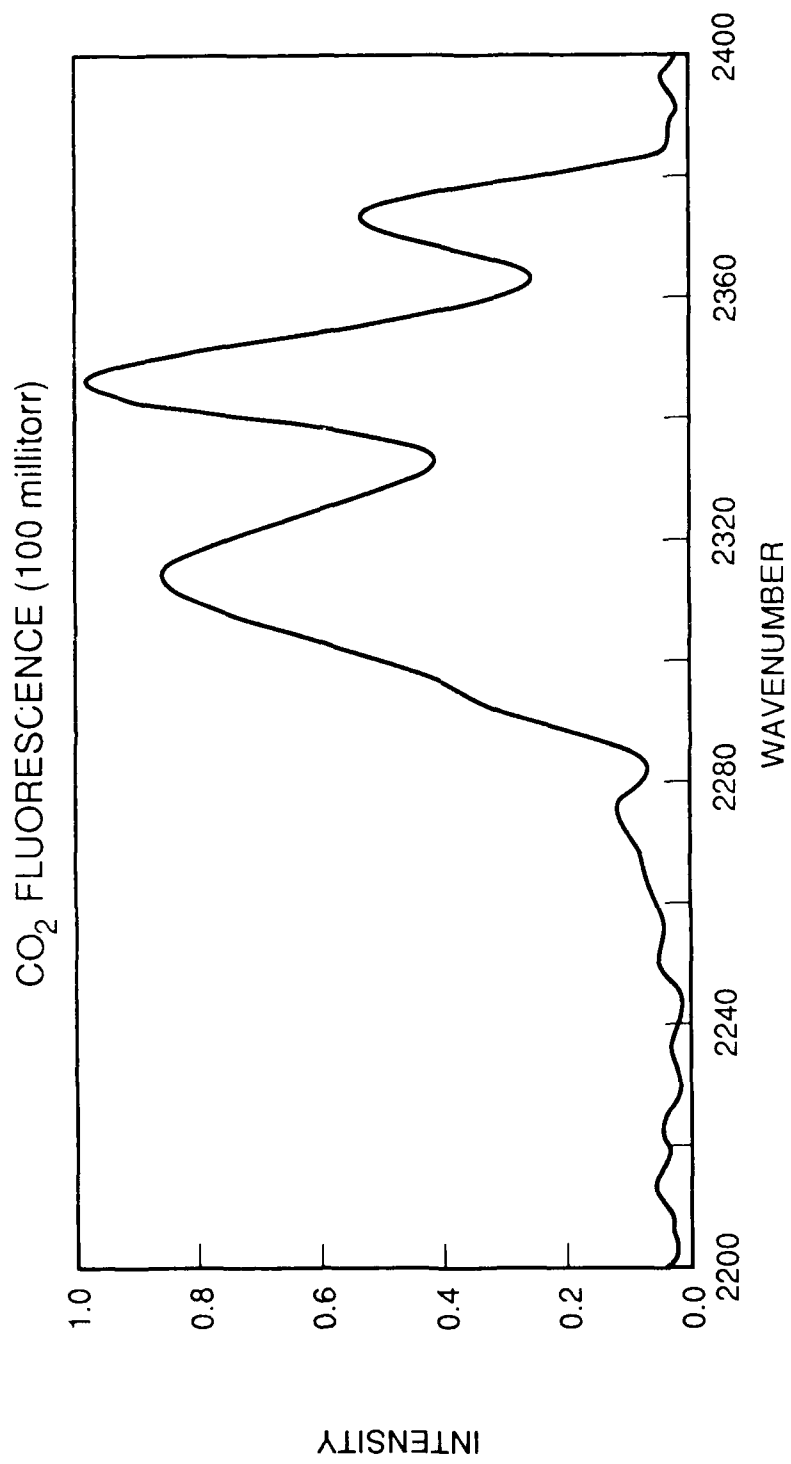


Figure 12. 0.1 t

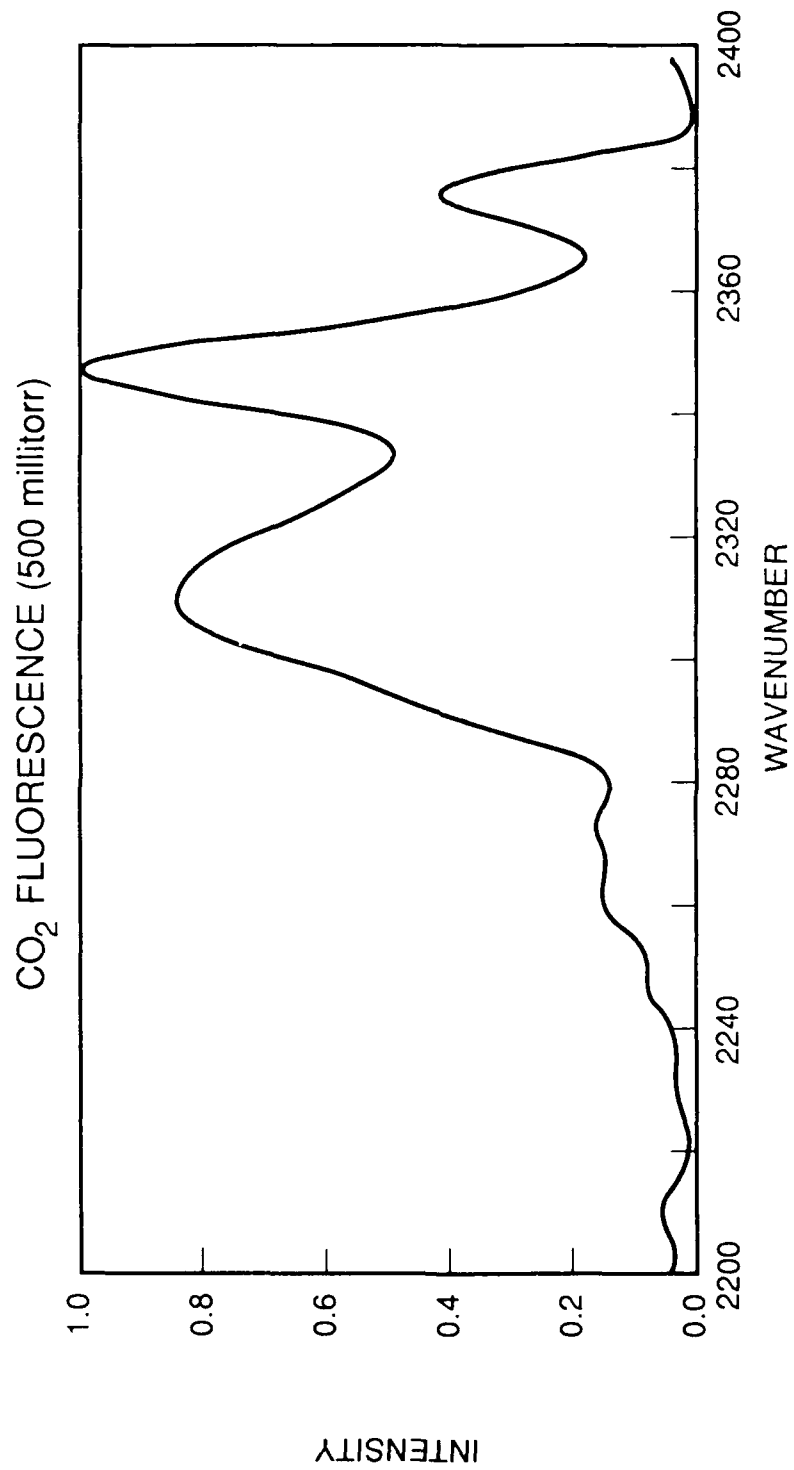


Figure 13. 0.5 t

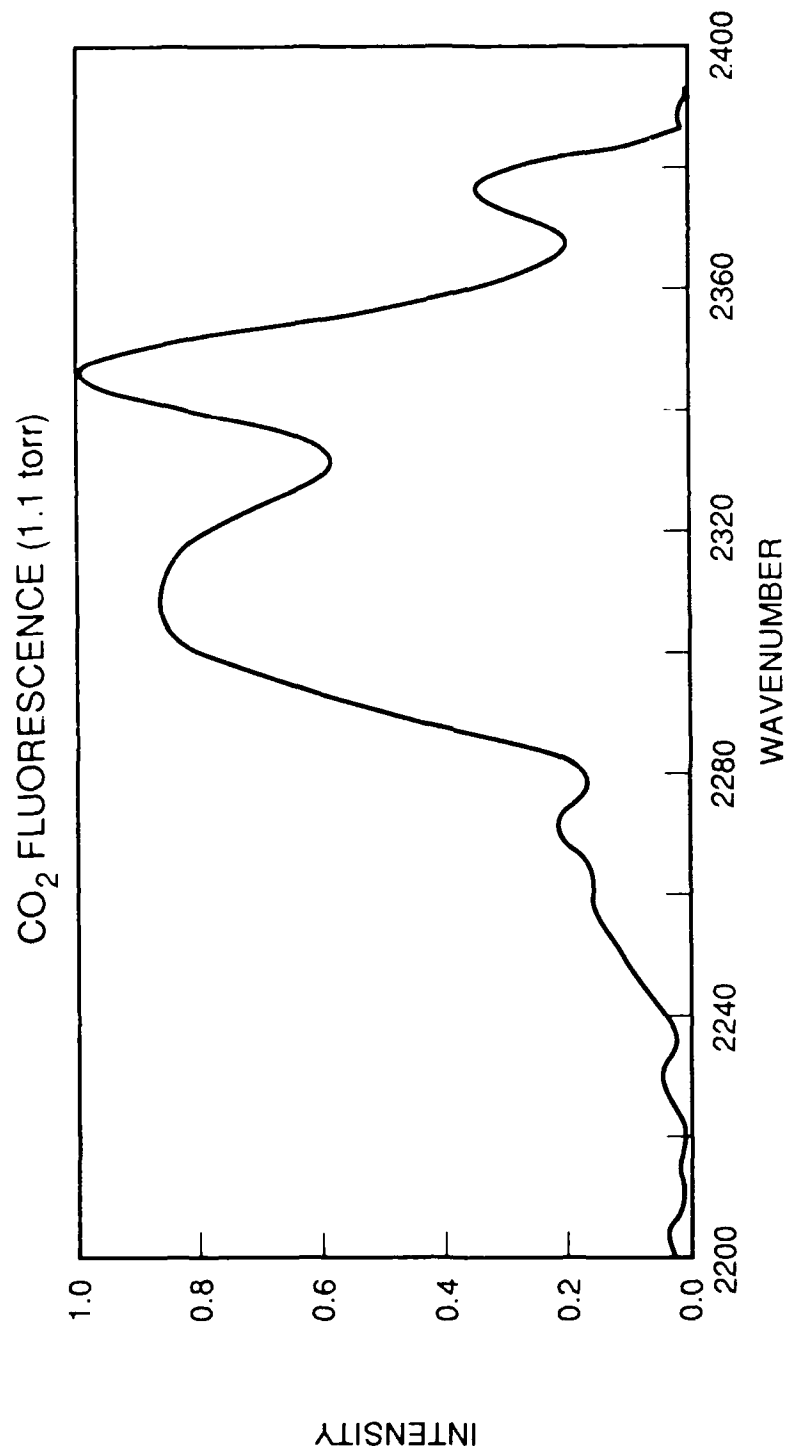


Figure 14. 1.1 t

Spectral Model of 4.3 micron CO₂ Fluorescence

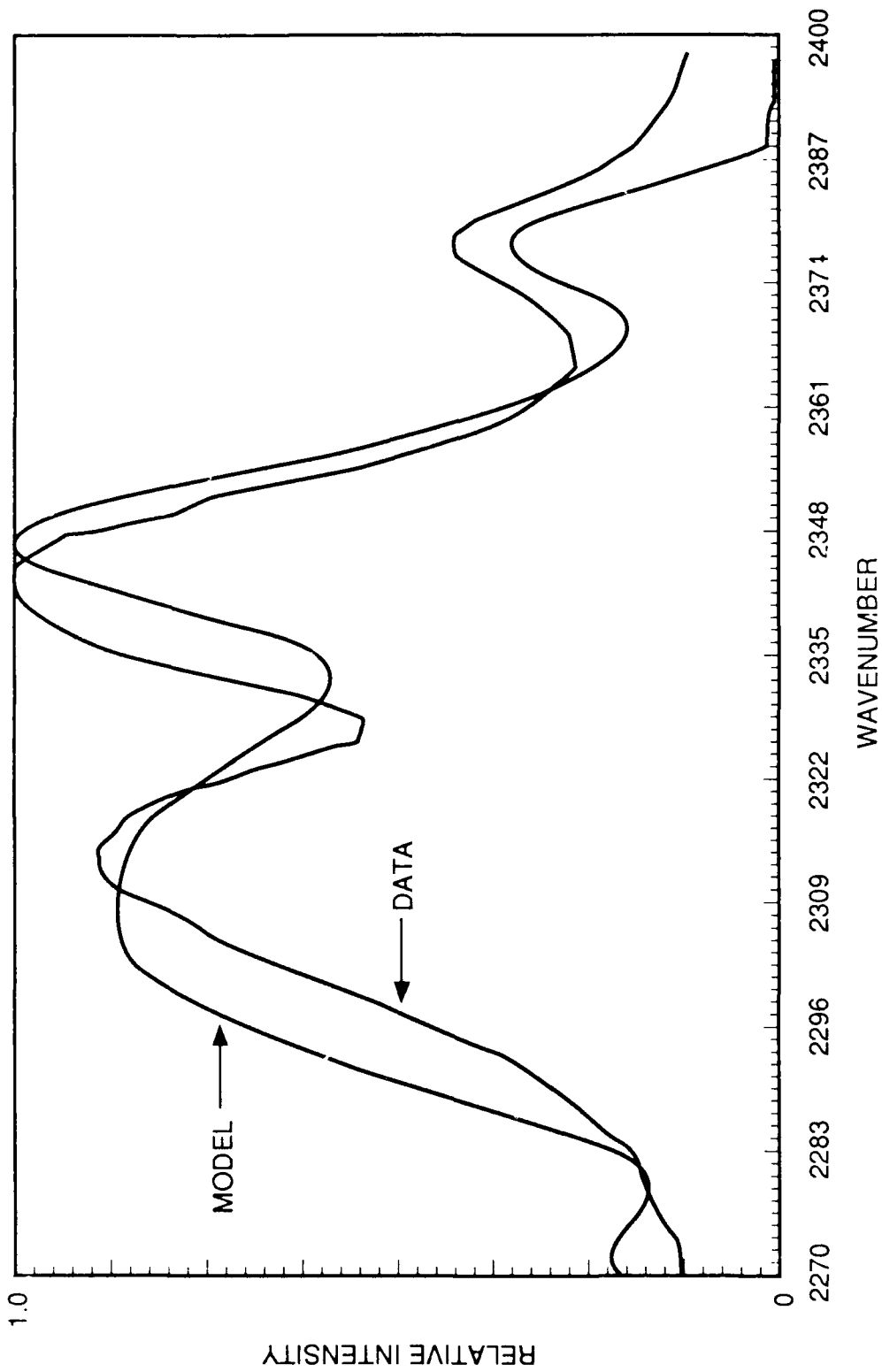


Figure 15. Spectral Fits

can in principle be solved by operating at pressures low enough to preclude significant collisional contributions, there is not enough signal at these levels to obtain the signal to noise ratio required to measure a 40:1 branching ratio. The alternative approach of deconvolving the relative contributions of the purely radiative components from those involving collisions is taken here.

Utilizing the results of the fluorescence excitation spectra an upper limit on the branching ratio can be established.

$$I_{4.3}/I_{2.7} \cdot \text{Bandpass Transmission (2.7)}/\text{BP Transmission (4.3)} \cdot D^*_{2.7}/D^*_{4.3} = 0$$

$$40 \text{ millivolts}/1.4 \text{ millivolts} \cdot 0.55/0.65 \cdot 5 \times 10^{10}/7.5 \times 10^{10} = 16.1 \pm 5$$

where $I_{4.3}$ ($I_{2.7}$) = peak intensity of the radiation passing through the 4.3(2.7) micron filter and D^* is the figure of merit for the InSb detector at the appropriate wavelength. This can only be considered an upper limit since an unknown portion of the 4.3 micron intensity is emitted from the 001 vibrational level populated through collisional processes. An estimate of this contribution is provided in the discussion of the interferometric data.

Examining the interferometric data in Figure 10, we can see that the spectrum is composed of at least 2 convolved vibrational bands at 4.3 microns and no signal above the noise at 2.7 microns. The spectral modeling does a fair job of determining the relative contributions to the 4.3 micron band. The major contributor to this band is the 021 → 020 transition, the band needed for the branching ratio measurement, while as much as a third of the integrated intensity is due to the 001 → 000 band. The fit can be made more accurate by adding contributions from both hot and isotopic bands. Assuming that the collisional energy transfer rate from the 021 band to the 001 band is 3×10^{-10} molecules-cm⁻²-sec⁻¹ and the radiative rate of the 021 band is 420 sec⁻¹, at the 1 torr pressure of CO₂ in the cell the ratio of 021 radiation to 001 radiation should be 2.33×10^4 . Some of this discrepancy can be accounted for by assuming that the nitrogen purge of the interferometer was ineffective at eliminating the CO₂ in the path of the fluorescence light. In this case, one must consider the optical thickness of all transitions connected to the ground state through a 50 cm path length of CO₂ with a partial pressure of 0.25 torr present in a standard atmosphere at sea level. Utilizing the appropriate line shape (Voigt profile), line strengths, and CO₂ pressures it was calculated that the integrated intensity of the 001 → 000 band radiation has been reduced by a factor of 1230 (see Table 1).

Table 1. Calculated Integrated Intensity of Vibrational Bands

	001 → 000 (4.3 μm)	021 → 000 (2.7 μm)
50 cm path to detector through interferometer	2.6	150
8 cm path to detector through filter	11.0	200
NO optical thickness	3200.00	230

This still leaves a discrepancy of approximately a factor of 20. Since the source of the nitrogen purge was liquid nitrogen boiloff it is unlikely that this could have enhanced the CO₂ concentration. The optical thickness calculations have been shown to work well in LABCEDE experiments and

performing the calculations using Doppler or Lorentzian line shapes cannot account for this discrepancy. This evidence together with the results of Reference 11 imply that the collision quenching rate of the 021 energy level should be reexamined.

The absence of signal above the noise in the 2.7 μm band prevents a direct branching ratio measurement. A lower limit of the $021 \rightarrow 020$ to $021 \rightarrow 000$ branching ratio can be established by examining the signal to noise ratio at 4.3 microns together with the effect of optical thickness on the $021 \rightarrow 000$ transition (column 2 of Table 1). The signal to noise ratio of the best 1 torr spectrum of CO_2 is 50:1. This scaled by the ratio of the interferometer response, response (4.3)/response (2.7) = 2.5 would indicate a lower limit branching ratio of CO_2 ($021 \rightarrow 020$)/ CO_2 ($021 \rightarrow 000$) ≥ 20 . Taking into account the optical thickness of the $021 \rightarrow 000$ transition reduces this lower limit to CO_2 ($021 \rightarrow 020$)/ CO_2 ($021 \rightarrow 000$) ≥ 13 . Thus this result, together with the results of the filtered fluorescence excitation experiment, brackets the branching ratio: $13 < \text{CO}_2$ ($021 \rightarrow 020$)/ CO_2 ($021 \rightarrow 000$) < 16.1 .

6. CONCLUSION

It can be concluded that the branching ratio of CO_2 ($021 \rightarrow 020$)/ CO_2 ($021 \rightarrow 000$) must be greater than 13 and less than 16. This is slightly smaller than the ratios of the Einstein coefficients and line strengths alone, but is unlikely to affect the results of the upper atmospheric CO_2 models. Just as important is the determination that Finzi and Moore's reaction coefficient for CO_2 (021) + CO_2 (000) \rightarrow CO_2 (001) + CO_2 (020) of $k = 3 \times 10^{-10}$ molecules $\cdot\text{cm}^{-2}\cdot\text{sec}^{-1}$ predicts a significantly different intensity¹³ ($\times 10$) ratio of CO_2 (021) \rightarrow CO_2 (020)/ CO_2 (001) \rightarrow CO_2 (000). It would be worthwhile to update Finzi's and Moore's experiment to confirm this number.

13. Finzi, J. and Moore, C.B. (1975) Relaxation of $\text{CO}_2(101)$, $\text{CO}_2(021)$, and $\text{N}_2\text{O}(101)$ vibrational levels by near-resonant V-V energy transfer, *J. Chem. Phys.* **63**:(6).

References

1. Stair, A.T., Jr., Ulwick, J.C., Baker, K.D., and Baker, D.J. (1975) Rocketborne observations of atmospheric infrared emissions in the auroral region, *Atmospheres of Earth and Planets*, ed. McCormac, B.M., Reidel, D., Dordrecht, Netherlands.
2. Kumer, J.B. (1974) *Analysis of 4.3 Micron ICE CAP Data*, Air Force Cambridge Res. Lab., Bedford, MA, AFCRL-TR-74-0334, ADA014847.
3. Sharma, R.D., Nadile, R., Stair, A.T., Jr., and Gallery, W. (1981) Earth limb emission analysis of Spectral Infrared Rocket Experiment (SPIRE) data at 2.7 micrometers, *Modern Utilization of Infrared Technology, Proc. Soc. Photo Opt. Instrum. Eng.* **304**:139-142.
4. Stair, A.T., Jr., Sharma, R.D., Nadile, R.M., Baker, D.J., and Grieder, W.F. (1985) Observation of limb radiance with cryogenic Spectral Infrared Rocket Experiment (SPIRE), *J. Geophys. Res.* **90**:(A10).
5. Kumer, J.B. (1977) Theory of the CO₂ 4.3 Aurora Related Phenomena, *J. Geophys. Res.* **82**:(16).
6. Sharma, R.D. (1985) CO₂ Component of Daytime Earth Limb Emission at 2.7 Micrometers, *J. Geophys. Res.* **90**:(A10).
7. James, T.C. (1976) *Laboratory Investigation of Infrared Fluorescence of CO₂*, HAES Report No. 60, Final Report to DNA 4238F, Cont. DNA 001-76-C-0017, ADA043524.
8. James, T.C. and Kumer, J.B. (1979) *Fluorescence Experimental and Auroral Data Evaluation to Improve Prediction of Nuclear Atmospheric Infrared Background*, DNA Report LMSC/D673384, ADA085724.
9. Bevington, P.R. (1969) *Data Reduction and Error Analysis for the Physical Sciences*, McGraw-Hill.
10. Rothman, L.S., and Young, L.D.G. (1981) Infrared Energy Levels and Intensities of Carbon Dioxide - II, *J. Quant. Spectrosc. Radiat. Trans.* **25**:505-524.
11. Caledonia, G.E., Green, B.D., and Murphy, R.E. (1982) On self-trapping of CO₂(v₃) fluorescence, *J. Chem. Phys.* **77**:(10).
12. Green, B.D., Caledonia, G.E., Piper, L.G., Goela, J.S., Fairbairn, A., and Murphy, R.E. (1981) *LABCEDE Studies*, AFGL-TR-82-0060, ADA114389.
13. Finzi, J. and Moore, C.B. (1975) Relaxation of CO₂(101), CO₂(021), and N₂O(101) vibrational levels by near-resonant V-V energy transfer, *J. Chem. Phys.* **63**:(6).